deduced from our STM study, and is not expected to be seen with experimental techniques that average over large surface areas. Our STM observations instead support a glassy state at the surface with medium-range order at room temperature.

Because a microscopic theory for STM experiments with a magnetic tip and sample is lacking, we can only speculate about the origin of the magnetic contrast observed at the atomic level. Magnetic dipole forces, although present, are not expected to lead to magnetic contrast on the atomic scale because of their long-range nature. Therefore, either spin-polarized tunneling or, less likely, the effect of magnetic exchange forces might be responsible for the observed contrast.

In summary, we have characterized the nanotopography and the atomic and magnetic surface structure of a well-known mineral by using STM with nonmagnetic as well as with magnetic sensor tips. The discovery of magnetic contrast at the atomic level allowed us to detect local order in the spatial distribution of the different magnetic ions Fe^{2+} and Fe^{3+} at the (001) surface of Fe$_3$O$_4$ at room temperature. We believe this study has proven that STM will become a most valuable tool in scientific research fields such as surface magnetism, transition metal oxides, and geology as well.

REFERENCES AND NOTES

1. G. Binnig, H. Rohrer, Ch. Gerber, E. Weibel, *Phys. Rev. Lett.* **49**, 57 (1982).
2. R. J. Hamers, *Annu. Rev. phys. Chem.* **40**, 531 (1989).
3. R. M. Feenstra, in *Scanning Tunneling Microscopy and Related Methods*, R. J. Behm, N. Garcia, H. Rohrer, Eds. (vol. 184 of *NATO ASI Series E: Applied Science*, Kluwer, Academic, Dordrecht, Holland, 1990), pp. 211–240.
4. R. J. Behm, *ibid.*, pp. 173–209.
5. H. F. Hess, R. B. Robinson, J. V. Waszczak, *Phys. B* **169**, 422 (1991).
6. R. V. Coleman *et al.*, *Adv. Phys.* **37**, 559 (1988).
7. D. M. Eigler and E. K. Schweizer, *Nature* **344**, 524 (1990).
8. D. M. Eigler, C. P. Lutz, W. E. Rudge, *ibid.* **352**, 600 (1991).
9. R. Wiesendanger, H.-J. Güntherodt, G. Güntherodt, R. J. Gambino, R. Ruf, *Phys. Rev. Lett.* **65**, 247 (1990).
10. R. Wiesendanger *et al.*, *J. Vac. Sci. Technol. B* **9**, 519 (1991).
11. R. Wiesendanger *et al.*, *Appl. Phys. A* **53**, 349 (1991).
12. R. Wiesendanger *et al.*, *Vacuum* **41**, 386 (1990).
13. R. Wiesendanger *et al.*, in preparation.
14. S. Iida *et al.*, *J. Appl. Phys.* **53**, 2164 (1982).
15. S. Iida, M. Mizoguchi, N. Goto, Y. Motomura, *J. Magn. Magn. Mater.* **31–34**, 771 (1983).
16. E. Kita, Y. Tokuyama, A. Tasaki, K. Siratori, *ibid.*, p. 787.
17. Financial support from the Swiss National Science Foundation is acknowledged.

23 September 1991; accepted 27 November 1991

Effects of High Temperature on Silicate Liquid Structure: A Multinuclear NMR Study

J. F. STEBBINS AND IAN FARNAN

The structure of a silicate liquid changes with temperature, and this substantially affects its thermodynamic and transport properties. Models used by geochemists, geophysicists, and glass scientists need to include such effects. In situ, high-temperature nuclear magnetic resonance (NMR) spectroscopy on ^{23}Na, ^{27}Al, and ^{29}Si was used to help determine the time-averaged structure of a series of alkali aluminosilicate liquids at temperatures to 1320°C. Isotropic chemical shifts for ^{29}Si increase (to higher frequencies) with increasing temperature, probably in response to intermediate-range structural changes such as the expansion of bonds between nonbridging oxygens and alkali cations. In contrast, isotropic chemical shifts for ^{27}Al decrease with increasing temperature, indicating that more significant short-range structural changes take place for aluminum, such as an increase in mean coordination number. The spectrum of a sodium aluminosilicate glass clearly indicates that at least a few percent of six-coordinated aluminum was present in the liquid at high temperature.

MOLTEN SILICATES ARE THE PRECURSORS of almost all igneous rocks (and therefore much of the earth's crust and mantle) and are the initial states of commercial glasses and glass-ceramics. Silicate melts are strongly bonded, partially ionic liquids, whose behavior is in many ways intermediate between those of organic molecular liquids and ionic molten salts (*1*). Most direct information about silicate liquid structure comes from studies of glasses, which contain configurations that are frozen in as temperature drops through the glass transition temperature T_g. However, large increases in heat capacity, thermal expansion, and compressibility on heating through T_g suggest that, above this point, significant structural changes occur with increasing temperature (*2*). Quantification of these changes is of key importance in understanding the properties of the liquids near and above their melting points, which are typically several hundred to more than 1000°C above T_g: high-temperature structure and dynamics control the properties of silicate liquids most relevant to geochemistry, geophysics, and materials science.

In situ high-temperature studies of vibrational (*3*) and x-ray absorption spectra (*4*) have indicated some details of the local structural changes that can take place with increasing temperature or on melting of silicates. Earlier work has shown that some temperature-induced liquid structural changes can be determined from NMR spectra of glass samples quenched at different rates and therefore recording different T_g values (*5, 6*). NMR has also been used to study ^{17}O, ^{23}Na, ^{27}Al, ^{29}Si, and other nuclides in silicate liquids at high temperature (*1, 7–11*). Most of this work has concentrated on the mechanism of the dynamic exchange among structural species at temperatures only a few hundred degrees above T_g. At higher temperatures, the NMR signals from all structural groups are fully averaged by rapid exchange and reorientation, even when that exchange involves breaking strong Si–O bonds (*7–10*). Recently, a systematic difference in isotropic chemical shifts for ^{27}Al between glasses and high-temperature liquids was recognized (*11*). These data suggested that changes in the average structure with temperature could be directly observed in the liquid state. From NMR data on a single nuclide, however, it has not been possible to determine the mechanism of these changes and relate them to thermodynamic properties. Some temperature effects, such as changes in bulk magnetic susceptibility, should cause similar perturbations in the NMR frequencies of different nuclides. Temperature-induced structural changes, on the other hand, could affect different nuclides similarly or dissimilarly, depending on their chemical behavior. We present here results from high-T NMR spectroscopy of ^{23}Na, ^{29}Si, and ^{27}Al that, taken together, place new constraints on the mechanism of temperature-induced structural change in silicate liquids.

We prepared a variety of alkali silicate and aluminosilicate glasses (*12*), chosen to minimize liquidus temperatures and viscosities and to allow simultaneous study of several nuclides (Table 1). In collecting the NMR data at room temperature, we used the

Department of Geology, Stanford University, Stanford, CA 94305.

Table 1. Sample compositions in nominal mole percent (*12*).

Sample	SiO_2	Al_2O_3	M_2O*	Gd_2O_3	NBO/(Si + Al)†
			M = *Li*		
LDS	66.7		33.3	0.03	1.0
L18A5	64.6	4.9	30.4	0.03	0.69
L18A5BU	64.6	4.9	30.4	0.0	0.69
L18A5BD	64.5	4.9	30.4	0.06	0.69
L40A5	37.0	4.1	58.9	0.02	2.43
			M = *Na*		
NDS	66.7		33.3	0.03	1.0
NDS10A1	62.5	6.2	31.3	0.03	0.67
			M = *K*		
KTS	80.0		20.00	0.04	0.5

*M_2O represents the alkali oxides as indicated. †NBO/(Si + Al) is the ratio of nonbridging O atoms to tetrahedral cations, neglecting nontetrahedral Si and Al, and assuming that alkali cations that charge-balance Al do not generate NBOs (*27*).

magic angle spinning (MAS) technique. At high temperatures on stationary samples, a probe developed in our laboratory and optimized for the accurate measurement of chemical shifts was used (*13*). When samples were heated to the liquid state at 1200° to 1300°C, ^{23}Na and ^{29}Si peaks narrowed to 150 to 400 Hz; ^{27}Al peaks remained relatively broad (1 to 4 kHz) and decreased in width with increasing temperature. The greater linewidth for the ^{27}Al peaks is probably due both to a combination of the great width of the total quadrupolar spectrum (at least several megahertz) with the relatively low mobility of this cation (when compared with Na^+) as well as to the very short ^{27}Al relaxation times in this temperature range. Single, Lorentzian lines were observed for all three nuclei in this temperature range.

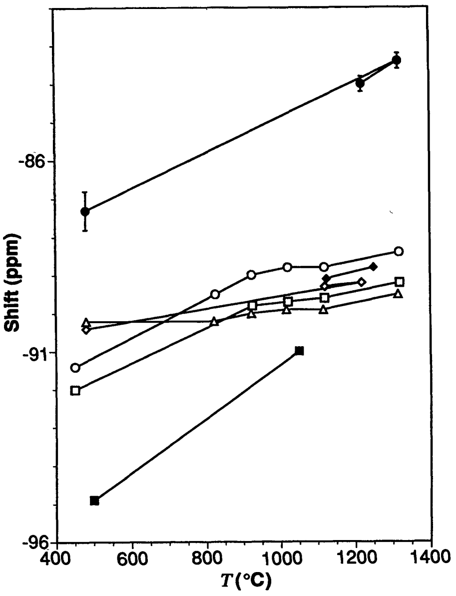

Fig. 1. ^{29}Si isotropic chemical shifts. MAS data (peak centroids) were collected at room *T* but are plotted at T_g. Open triangles, L18A5-2; open diamonds, L18A5BD-1; closed diamonds, L18A5BU-1; closed circles, NDS10A1-3; open circles, NDS-1; open squares, LDS-1; closed squares, KTS (+6 ppm to bring on-scale). Typical error bars are shown for one composition. Uncertainties in *T* and T_g are smaller than the size of the symbols. Not included in the plot are two points for the low-silica composition L40A5-4 at −73.5 ppm collected at 1215° and 1315°C.

Isotropic chemical shifts (δ_{iso}) for ^{29}Si in both liquids and glasses are shown in Fig. 1. As expected from extensive earlier work on glassy and crystalline silicates (*14*), liquids higher in the network-forming components SiO_2 and $MAlO_2$ have more negative (lower frequency) values of δ_{iso}. Shifts for Na-bearing samples are less negative (higher frequency) than for corresponding Li samples, as expected from the smaller size and greater electronegativity of Li. For most of the samples, a small but significant increase in shift was observed at higher temperature that became obvious when results were compared with the MAS data, such that $d\delta/dT > 0$ (Fig. 2).

In the ambient-temperature MAS and static spectra for ^{27}Al (Figs. 3 and 4), the main peaks (due to the central, 1/2 to −1/2 transition) are shifted to frequencies lower than δ_{iso} by second-order quadrupolar perturbations. As samples were heated above T_g, the peaks generally became more symmetrical and narrower as rotation and chemical exchange began to occur at rates on the order of this perturbation (several kilohertz). At higher temperatures, a shift toward higher frequencies occurred as the viscosities of the liquids became low enough such that complete averaging over all transitions occurred (Fig. 5). This averaging requires more than just local motion of the Al cations and implies that rapid exchange of first-neighbor cations also was taking place (*15*). Strong Si–O and Al–O bonds must therefore be breaking and reforming at the 10^0- to 10^2-MHz time scale at these temperatures. This is indeed expected from the known viscosities of the liquids. For example, at 1300°C, samples NDS10A1 and L18A5 have viscosities of about 10 Pa-s (*16*), which correspond to shear relaxation rates of about 1000 MHz (*17*). We have shown that such bulk rates correspond closely to rates of local Si–O bond breaking as determined from ^{29}Si NMR line shapes (*1*). Similar conclusions have recently been drawn from data in the Al_2O_3-SiO_2 and CaO-Al_2O_3 systems (*18*).

In contrast to the temperature effect on δ_{iso} for ^{29}Si, further increases in temperature generally moved fully averaged ^{27}Al peaks to slightly lower frequencies ($d\delta/dT < 0$). Such shifts are most obvious when liquid data are compared with estimates for δ_{iso} from the MAS spectra (Fig. 5). The systematic decrease in shift from glasses to corresponding liquids noted in a recent study is thus confirmed (*11*). A much smaller effect in the same direction is apparent in the ^{23}Na data for one liquid (Fig. 5). This finding and the opposite signs of the temperature effects on ^{27}Al and ^{29}Si shifts indicate that changes in bulk magnetic susceptibility do not dominate, as these would influence frequencies for all three nuclides similarly.

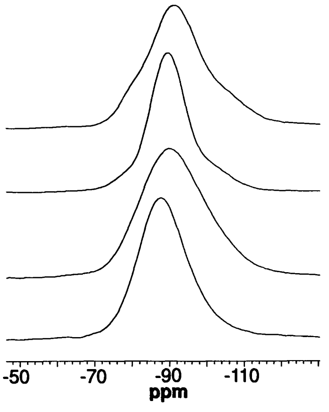

Fig. 2. ^{29}Si MAS spectra for glasses after high-*T* NMR experiments. Data for KTS have appeared previously (*24*). Spinning rates of 6 to 7 kHz were used, with 10,000 to 20,000 pulses, 30° rf tip angle, and 1-s delays between pulses. From top to bottom, data are for LDS-1, NDS-1, L18A5BD-1, and NDS10A1-3. Shoulders on the main Q^3 peaks show the presence of significant amounts of Q^2 and Q^4 species in the lithium and sodium disilicate glasses (LDS and NDS) (*5*, *8*, *25*), with LDS containing a more disordered distribution (*26*). Addition of Al results in an increase in the range of local geometries at Si sites and a corresponding peak broadening. Sample L18A5BD shows a greater range of shifts than the corresponding Na sample, NDS10A1, which is also consistent with greater disorder.

The ^{27}Al MAS spectra for samples

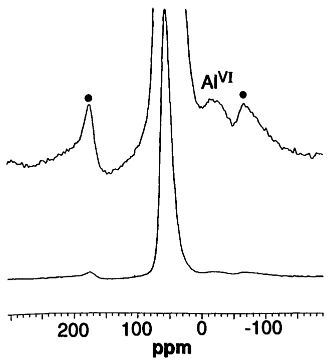

Fig. 3. Background-subtracted ^{27}Al MAS spectrum for NDS10Al-2 glass, after high-*T* NMR experiments. Data from about 10^5 30° pulses (400 ns), with a 0.2-s delay, were averaged. A spinning speed of about 12 kHz was used. Solid circles mark spinning side bands for the 1/2 to −1/2 peak, and the peak probably due to Al^{VI} is labeled. The resolution of this peak is slightly enhanced by subtraction of broad background component. The upper spectrum is plotted with the vertical scale enlarged ten times.

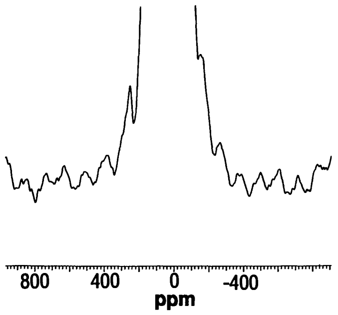

Fig. 4. ^{27}Al MAS spectrum for NDS10A1-2 glass plotted to show spinning side bands for 1/2 to 3/2 transitions. Conditions are similar to those in Fig. 5, except that the spinning speed was 10 kHz and about 2×10^5 pulses were used.

NDS10A1-2 and L18A5BU-2 (of similar SiO_2 and Al_2O_3 contents) are similar to each other (Fig. 3). The main peaks are asymmetrical with tails toward lower frequency and are clearly attributable to Al coordinated by four oxygens (Al^{IV}). As for ^{29}Si, the full width at half maximum of the ^{27}Al spectrum for the Li-bearing sample (about 3 kHz) is considerably greater than that for the Na sample (2.2 kHz), probably again because of greater disorder. The narrower peak for NDS10A1-2 allowed resolution of a small second peak at about −10 ppm (Fig. 3). Given well-known correlations between peak positions and coordination number for ^{27}Al (*14*), this peak indicates that a small amount of Al coordinated by six oxygens (Al^{VI}) is present, comprising about 1 to 3% of the total central peak area. We cannot rule out the presence of a similar or perhaps somewhat greater amount of Al^{V}, which could be hidden by the tail of the main Al^{IV} peak.

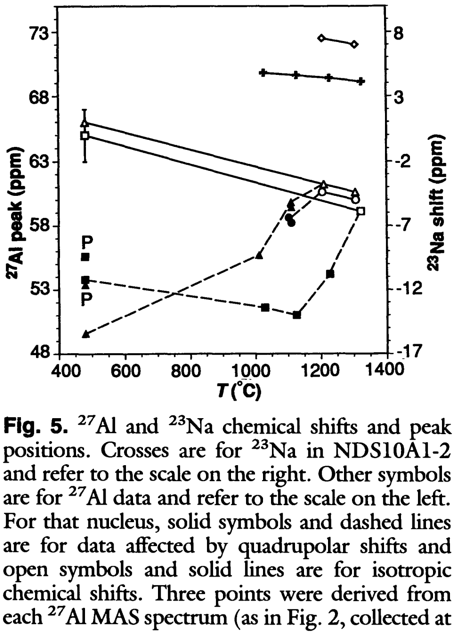

Fig. 5. ^{27}Al and ^{23}Na chemical shifts and peak positions. Crosses are for ^{23}Na in NDS10A1-2 and refer to the scale on the right. Other symbols are for ^{27}Al data and refer to the scale on the left. For that nucleus, solid symbols and dashed lines are for data affected by quadrupolar shifts and open symbols and solid lines are for isotropic chemical shifts. Three points were derived from each ^{27}Al MAS spectrum (as in Fig. 2, collected at room *T* but plotted at T_g): P indicates MAS central peak maxima; solid symbols are centroids of 1/2 to −1/2 transition; open symbols are isotropic shifts estimated on the basis of spinning side bands of satellite transitions. Typical error bars are shown for estimated isotropic shifts in the glasses; error estimates for other data are similar in size to the symbols. Diamonds, L40A5-1; triangles, L18A5BU-2; circles, L18A5-1; squares, NDS10A1-2.

Structural effects on chemical shifts for ^{29}Si and ^{27}Al in silicates are generally similar, although they tend to be somewhat smaller for the latter (*14*). The largest changes in δ are caused by changes in the number of first-neighbor anions: increasing coordination number systematically decreases δ. Smaller effects in the same direction result from the substitution of more electronegative or smaller first-neighbor cations (for example, Al^{3+} or Li^+ for Na^+) and from increases in angles between tetrahedra. All of these changes are linked to the same underlying mechanism, which is an increase in the ionic character of the Si–O or Al–O bond and an increase in the net positive charge on Si or Al (*14*).

Small amounts of Si^V are present in $K_2Si_4O_9$ glass, and the abundance of this species increases with increasing temperature (*6*). The predicted change in the abundance of Si^V between T_g and 1300°C (a few tenths of 1%) would lead to a decrease in δ for ^{29}Si of a few tenths of 1 ppm. The observed change in δ over this temperature interval is much larger and of the opposite sign. Structural effects other than changes in coordination number thus must dominate. A likely cause of the increase in δ with temperature for ^{29}Si is an increase in the lengths of bonds between nonbridging O atoms and network modifier M^+ cations, which should mimic the compositional effect of substitution of a larger cation. Similar effects of both composition and temperature have been noted in a number of NMR studies of ^{205}Th in molten salts (*19*). In silicates, this kind of structural change is expected from the commonly suggested mechanism of thermal expansion, in which volume changes are in large part accommodated by the lengthening of the relatively weak O–M bonds. It is possible that an increase in O–M distances of this sort results in a relaxation and an actual shortening of the Si–O distance with increasing temperature, as has been observed in crystalline silicates (*20*).

At these compositions Al is a dilute species and thus should have first-neighbor cations similar to Si, perhaps with a somewhat higher average number of Si neighbors (*21*). Effects on chemical shifts caused by the intermediate-range structural changes noted in the previous paragraph are therefore expected to be similar for ^{29}Si and ^{27}Al. The fact that the observed temperature effects for the two nuclides are opposite to each other suggests that for Al some change in the short-range structure occurs that is more significant than that for Si. Al cations are larger than Si cations and generally have less net positive charge. Therefore, Al–O bonds are generally weaker than Si–O bonds and, like O–M^+ bonds, may lengthen with increasing temperature. This could contribute both to the overall thermal expansion and to the observed decrease in ^{27}Al chemical shift. If Al–O bonds lengthen sufficiently, the coordination sphere of some Al cations could expand to include more than four oxygens. Even if such Al^V or Al^{VI} sites are short-lived, their presence will further contribute to the negative $d\delta/dT$. The contribution of the mixing of different cation coordinations to the configurational entropy should also favor the formation of new types of Al sites at high *T*. In addition, Si and Al cations with extra O neighbors have often been suggested as transition states in viscous flow in silicate liquids, and their increased abundance may be one factor that reduces the viscosity of these highly structured liquids with increasing temperature (*1, 6*).

The presence of Al with a high coordination number in silicate liquids has long been a controversial issue in geochemistry and glass science. MAS NMR has recently provided the first substantive evidence that both Al^V and Al^{VI} do exist in glasses in the Al_2O_3-SiO_2 binary system and in the CaO-Al_2O_3-SiO_2 ternary system (*22, 23*). Our data showing an Al^{VI} peak in the MAS spectrum for NDS10A1 confirm that at least the latter species exists in an alkali aluminosilicate composition, even when the mole fraction of Na greatly exceeds that of Al. The increase in the Al^{VI} content needed to explain the observed change in ^{27}Al chemical shifts over the *T* range from T_g to 1300°C (reaching a value of perhaps 7 to 10%) is of the order expected if the enthalpy for the formation of this species is similar to that estimated for Si^V [about 20 kJ/mol (*6*)]. Although we have not been able to directly observe Al^V in these glasses, its formation at high temperature would also cause ^{27}Al shifts to move in the observed direction. This process is suggested by earlier results on Si^V (*6*) and by variable quench rate experiments on glasses in the Al_2O_3-SiO_2 binary system (*23*). It is, of course, not possible to uniquely interpret a single average measure of the structure (δ_{iso}), but Al coordination change with temperature is consistent with multinuclear NMR data on both liquids and glasses. Future experiments such as spectroscopy on glasses with different glass transition temperatures should be able to test this hypothesis and further quantify the abundances of structural species.

REFERENCES AND NOTES

1. I. Farnan and J. F. Stebbins, *J. Am. Chem. Soc.* **112**, 32 (1990); J. F. Stebbins, I. Farnan, X. Xue, *Chem. Geol.*, in press.
2. P. Richet, *Geochim. Cosmochim. Acta* **48**, 471 (1984).
3. B. O. Mysen, *J. Geophys. Res.* **95**, 15733 (1990); F. A. Seifert, B. O. Mysen, D. Virgo, *Geochim. Cosmochim. Acta* **45**, 1879 (1981).
4. G. A. Waychunas, G. E. Brown, Jr., C. W. Ponader, W. E. Jackson, *Nature* **332**, 251 (1988); W. E. Jackson, thesis, Stanford University (1991).
5. M. E. Brandriss and J. F. Stebbins, *Geochim. Cosmochim. Acta* **52**, 2659 (1988).
6. J. F. Stebbins, *Nature* **351**, 638 (1991).
7. ______, J. B. Murdoch, A. Pines, I. S. E. Carmichael, *ibid.* **314**, 250 (1985); J. F. Stebbins, E. Schneider, J. B. Murdoch, A. Pines, I. S. E. Carmichael, *Rev. Sci. Instrum.* **57**, 39 (1986); S.-B. Liu, A. Pines, M. Brandriss, J. F. Stebbins, *Phys. Chem. Minerals* **15**, 155 (1987); S.-B. Liu, J. F. Stebbins, E. Schneider, A. Pines, *Geochim. Cosmochim. Acta* **52**, 527 (1988); J. F. Stebbins, I. Farnan, P. Fiske, *Eos* **72**, 572 (1991).
8. J. F. Stebbins, *J. Non-Cryst. Solids* **106**, 359 (1988).
9. S. Shimokawa *et al.*, *Chem. Lett.* **1990**, 617 (1990).
10. F. Taulelle, J. P. Coutures, D. Massiot, J. P. Rifflet, *Bull. Magn. Reson.* **11**, 318 (1989); D. Massiot, F. Taulelle, J. P. Coutures, *Colloq. Phys.* **51**, C5-425 (1990).
11. B. Coté, D. Massiot, F. Taulelle, J. P. Coutures, abstract, 4th Silicate Melt Workshop, Le Hohwald, France, 1991; B. T. Poe *et al.*, *Eos* **72**, 572 (1991).
12. The nominal compositions of samples studied, before high-*T* NMR runs, are listed in Table 1. Errors for major elements are about ±1% relative, for Gd_2O_3 about 20% relative. All but one contained a small amount of a paramagnetic impurity (Gd_2O_3) added to decrease ^{29}Si relaxation times. Samples were synthesized from reagent-grade alkali carbonates, $Al(OH)_3$, Gd_2O_3, and SiO_2. Si at natural isotopic abundance was used. Each sample listed in Table 1 was synthesized separately. Hyphenated sample numbers (for example, NDS-1) in text and figures indicate different portions of the same batch. Glasses both before and after high-*T* experiments were shown by ^{29}Si NMR and optical microscopy to be crystal-free. Only sample L40A5 could not readily be quenched to a glass. Minor changes in composition during high-*T* NMR experiments (primarily due to a small amount of contamination from the BN sample capsules) were noted by small differences in MAS peak positions between starting glasses and those quenched from high-*T* NMR runs (0.3 to 0.4 ppm more shielded), by semiquantitative ^{11}B MAS spectra (showing up to about 1% B_2O_3), and by small changes in high-*T* peak positions during relatively long runs (0.2 to 0.4 ppm). None of these significantly affect conclusions, but for consistency some data collected during relatively slow initial heating of the liquids have been omitted from the figures. Alkali loss during NMR experiments is insignificant for the large samples (0.3 to 0.7 g) and the short run durations used here.
13. NMR spectra were recorded with a Varian VXR 400S spectrometer. High-*T* data were collected with a home-built probe [J. F. Stebbins, *Chem. Rev.* **91**, 1353 (1991)]. The sample and radio-frequency (rf) coil were resistively heated in a small, water-cooled furnace with vertical Mo wire windings, blanketed by N_2–3% H_2 gas. Temperatures were controlled by a thermocouple in the furnace windings that we calibrated before the NMR runs by placing a second thermocouple in a sample container in the rf coil and are accurate to about 5°C. The only possible instrumental source of variation in NMR resonant frequency with *T* is perturbation of the magnetic field at the sample caused by the current flow in the heater. This effect is minimized by careful, noninductive winding. We routinely measured and corrected residual field shifts of 1 to 3 ppm by collecting data with heater current flowing in opposite directions, and these shifts introduce uncertainties of about 0.2 ppm in measured chemical shifts. Spectra were recorded at 79.4 MHz for ^{29}Si, 104.2 MHz for ^{27}Al, and 105.8 MHz for ^{23}Na. For ^{29}Si high-*T* spectra, data from 1000 to 2000 pulses, requiring about 5 min to collect, were averaged. For ^{27}Al and ^{23}Na, 100 to 400 pulses were used, requiring less than 1 min. Signal to noise ratios for ^{23}Na, ^{27}Al, and ^{29}Si were typically at least 100:1, 50:1, and 10:1, respectively. For these nuclei, samples of 1 M NaCl, 1 M $Al(NO_3)_3$, and pure $Si(CH_3)_4$ were run at ambient *T* as frequency references. For ^{27}Al, 90° pulse times were measured at high *T*, and comparison with results for crystalline Al_2O_3 showed that liquid spectra collected above about 1200°C were fully averaged over all transitions. Under these conditions, peaks for ^{23}Na and ^{27}Al were accurately fitted by single Lorentzians, and dispersion versus absorption (DISPA) plots were circular. Both indicate that exchange dynamics were rapid enough to eliminate dynamic quadrupolar line shifts [L. G. Werbelow, *J. Chem. Phys.* **70**, 5381 (1979); ______ and A. G. Marshall [*J. Magn. Reson.* **43**, 443 (1981)]. MAS data were collected with a commercial high-speed probe. Spinning rates of about 6 kHz for ^{29}Si (Al_2O_3 rotors) and up to 12 kHz for ^{27}Al (ZrO_2 rotors) were used in a probe from Doty Scientific. Acquisition delays were chosen to eliminate any effects of differential relaxation rates on peak shapes. We subtracted a significant ^{27}Al background from the probe by collecting data with an empty rotor under conditions identical to those for glass samples. For ^{29}Si and the central (1/2 to −1/2) transition for ^{27}Al, MAS peak centroids were determined that included the first set of spinning side bands. For ^{27}Al, the centroid of the 1/2 to 3/2 transition spinning side-band manifold was estimated from side-band peak centers and used in conjunction with the main peak to estimate isotropic chemical shifts in the glasses [H. J. Jacobsen, J. Skibsted, H. Bildsoe, N. C. Nielsen, *J. Magn. Reson.* **85**, 173 (1989); E. Lippmaa, A. Samosen, M. Mägi, *J. Am. Chem. Soc.* **108**, 1730 (1986)]. The relatively low intensity of the satellite side bands introduced an uncertainty of about 3 ppm in this estimation. We compared data for Gd-doped and undoped samples of the same lithium aluminosilicate composition (L18A5BD and L18A5BU). ^{29}Si and ^{27}Al NMR line shapes in both liquid and glass samples were the same, and peak positions differed by less than 0.5 ppm.
14. For review, see G. Engelhardt and D. Michel, *High-Resolution Solid-State NMR of Silicates and Zeolites* (Wiley, New York, 1987).
15. Stoichiometry requires about one nonbridging O per tetrahedral cation in most of the compositions studied. This does not allow for time-averaged local symmetry to be increased to cubic (reducing the electric field gradient to 0) simply by local motion of the cations around their mean positions.
16. Y. Bottinga and D. F. Weill, *Am. J. Sci.* **272**, 438 (1972).
17. D. B. Dingwell and S. L. Webb, *Phys. Chem. Minerals* **16**, 508 (1989).
18. P. F. McMillan, B. T. Poe, B. Coté, D. Massiot, J. P. Coutures, *Eos* **72**, 572 (1991).
19. S. Hafner and N. H. Nachtrieb, *J. Chem. Phys.* **40**, 2891 (1964); Y. Nakamura, Y. Kitazawa, M. Shimoji, S. Shimokawa, *J. Phys. Chem.* **87**, 5117 (1983).
20. R. M. Hazen, in *Microscopic to Macroscopic*, S. W. Kieffer and A. Navrotsky, Eds. (Mineralogical Society of America, Washington, DC, 1985), pp. 317–346.
21. This assumption might not be the case if there was extensive clustering of Al polyhedra. There is not clear evidence that this occurs in these compositions. In tectosilicate glass compositions, NMR studies have suggested that Al and Si distributions are random [see (*14*)].
22. S. H. Risbud, R. J. Kirkpatrick, A. G. Taglialavore, B. Montez, *J. Am. Ceram. Soc.* **70**, C10 (1987); R. K. Sato, P. F. McMillan, P. Dennison, R. Dupree, *Phys. Chem. Glasses* **32**, 149 (1991).
23. R. K. Sato, P. F. McMillan, P. Dennison, R. Dupree, *J. Phys. Chem.* **95**, 4484 (1991).
24. X. Xue, J. F. Stebbins, M. Kanzaki, P. F. McMillan, B. Poe, *Am. Mineral.* **76**, 8 (1991).
25. J. B. Murdoch, J. F. Stebbins, I. S. E. Carmichael, *ibid.* **70**, 332 (1985).
26. For a Si site with four O neighbors, the number of O atoms bonded to other network-forming cations (Si^{IV}, Al^{IV}, and so forth) is indicated by *n* in Q^n.
27. B. O. Mysen, *Structure and Properties of Silicate Melts* (Elsevier, Amsterdam, 1988).
28. Supported under National Science Foundation grants EAR 85-53024 and EAR 89-05188. We thank B. Coté, J. P. Coutures, D. Massiot, P. McMillan, and F. Taulelle for useful discussions; P. Fiske for help with sample preparation; and two anonymous reviewers for helpful comments.

23 September 1991; accepted 19 November 1991

Experimental Phylogenetics: Generation of a Known Phylogeny

David M. Hillis, James J. Bull, Mary E. White,
Marty R. Badgett, Ian J. Molineux

Although methods of phylogenetic estimation are used routinely in comparative biology, direct tests of these methods are hampered by the lack of known phylogenies. Here a system based on serial propagation of bacteriophage T7 in the presence of a mutagen was used to create the first completely known phylogeny. Restriction-site maps of the terminal lineages were used to infer the evolutionary history of the experimental lines for comparison to the known history and actual ancestors. The five methods used to reconstruct branching pattern all predicted the correct topology but varied in their predictions of branch lengths; one method also predicts ancestral restriction maps and was found to be greater than 98 percent accurate.

The development over the past four decades of explicit methods for phylogenetic inference (*1*) has permitted biologists to reconstruct the broad outlines of evolutionary history and to interpret comparative biological studies within an evolutionary framework (*2*). However, evolutionary history usually cannot be observed directly, at least over the course of relevant magnitudes of change, so that assessment of phylogenetic methods has relied on numerical simulations. Although simulations have provided considerable insight into the effectiveness of various

---

Departments of Zoology and Microbiology, University of Texas, Austin, TX 78712.